Thin Solid Films 589 (2015) 730–734

Contents lists available at ScienceDirect

Thin Solid Films

journal homepage: www.elsevier.com/locate/tsf

Electrical transport properties of V_2O_5 thin films obtained by thermal annealing of layers grown by RF magnetron sputtering at room temperature

H.M.R. Giannetta [a,b,*], C. Calaza [d], D.G. Lamas [c], L. Fonseca [d], L. Fraigi [a,b]

[a] Centro de Micro y Nano Electrónica del Bicentenario (CMNB), Instituto Nacional de Tecnología Industrial (INTI), San Martín, Buenos Aires, Argentina
[b] Universidad Tecnológica Nacional (UTN) — Facultad Regional Buenos Aires (FRBA), Argentina
[c] Universidad Nacional del Comahue CONICET-CITEFA — Laboratorio de Caracterización de Materiales, Facultad de Ingeniería, Neuquen, Argentina
[d] Instituto de Microelectrónica de Barcelona, Centro Nacional de Microelectrónica (IMB-CNM, CSIC), Campus UAB, Bellaterra, 08193 Barcelona, Spain

ARTICLE INFO

Article history:
Received 25 March 2015
Received in revised form 28 May 2015
Accepted 29 June 2015
Available online 3 July 2015

Keywords:
V_2O_5 thin film
Small polaron hopping
RF magnetron sputtering
Thin solid films

ABSTRACT

The present study investigates the main electrical transport mechanism in V_2O_5 thin films deposited by RF magnetron sputtering on the basis of the Mott's small polaron hopping model. The material under test was obtained at room temperature from a V_2O_5 target and then oxidized at high temperature under air atmosphere to obtain the desired V_2O_5 phase. The dependence of the electrical conductivity of the V_2O_5 thin films with temperature was analyzed using the Mott's small polarons hopping transport model under the Schnakenberg form. Model results suggest a polaron binding energy $W_H = 0.1682$ eV, with a structural disorder energy $W_D = 0.2241$ eV and an optical phonon frequency $\nu_0 = 0.468 \times 10^{13} s^{-1}$. These results are in agreement with data reported in literature for single crystal V_2O_5. However, the carrier mobility $\mu = 1.5019 \times 10^{-5}$ cm^2/Vs computed in the non-adiabatic regime is significantly smaller than that of the single crystal, suggesting a strong electron–phonon coupling in the V_2O_5 thin films obtained with the proposed deposition method.

1. Introduction

Vanadium is a transition metal element having a large amount of oxide phases due to its multi-valent character (V^{+2}, V^{+3}, V^{+4}, V^{+5}), being the vanadium pentoxide (V_2O_5, one of the Wadsley phases with $V_{2n}O_{5n-2}$ stoichiometric formula [1]) the most stable one. V_2O_5 is a wide band gap *n*-type semiconductor material [2] with particularly useful properties due to the fact that charge transport is performed by means of polarons, as has been reported for both the bulk single-crystal structure [3], and the amorphous V_2O_5 layers [4,5]. These properties make V_2O_5 thin films candidate for many practical uses, such as a catalyst material in gas sensors [6,7], as a dielectric constituent material in super capacitors [8], as a high capacity storage medium in Li-ion batteries, as a cathode in these batteries [9], or as a thermo-resistive material in thermal infrared detectors [10]. V_2O_5 thin films can be prepared using various deposition techniques [11], being sputtering the preferred method due to the good surface uniformity provided. In present work the V_2O_5 thin films were obtained by means of a two step process, which is intended to make the film deposition compatible with a low temperature lift-off patterning process. First a thin film is deposited at room temperature by RF magnetron sputtering from a VO_2 target. After the lift-off patterning the film is oxidized at high temperature under air atmosphere to obtain the desired V_2O_5 phase. The following sections illustrate the method used to obtain the films, the morphological and structural characterization carried out with the different samples, and the electrical measurements performed. Finally, the electrical conductivity dependence with temperature is analyzed using the model proposed by Mott [12,13] for the charge transport performed by small polarons hopping, under the Schnakenberg formulation [14].

2. Methods and materials

The proposed V_2O_5 thin films compatible with the lift-off patterning process were obtained in two steps. Initially, a VO_x thin film was deposited on top of a Si(100) wafer pre-coated with a dielectric layer by means of RF magnetron sputtering, using a high purity (99.9%) VO_2 target material. The deposition process was performed at room temperature using a base pressure of 10^{-5} mBar, a RF plasma power of 200 W, and an Argon flow of 20 sccm. Based on the changes in the Gibbs free energy linked to the different vanadium oxide stable phases [15], it is known that for temperatures higher than 434 °C the different stable phases arise following the $VO_2 \rightarrow VO \rightarrow V_2O_3 \rightarrow V_2O_5$ sequence. Therefore, to end up with a single phase V_2O_5 film the samples were subjected to a subsequent thermal annealing at 475 °C in air for 3 h, to promote

* Corresponding author at: Centro de Micro y Nano Electrónica del Bicentenario (CMNB), Instituto Nacional de Tecnología Industrial (INTI), San Martín, Buenos Aires, Argentina.
E-mail addresses: hgiann@inti.gov.ar, hgiannetta@electron.frba.utn.edu.ar (H.M.R. Giannetta).

http://dx.doi.org/10.1016/j.tsf.2015.06.048
0040-6090/

the complete oxidation of the layer until the final stable phase. The morphological characterization of the processed samples was performed by means of field emission scanning electron microscopy (FE-SEM, Zeiss Supra 40), making use of a low acceleration potential 3 kV to prevent charging of the films. All samples were analyzed using the same magnification level in order to make a fair comparison of the surface morphology and grain arrangement. The structural characterization was performed by X-ray diffraction, using a cathode Cu(Kα) = 1.5418 Å (XRD-Philips PW 3710) configured in glancing angle geometry, and a cathode Cu(Kα) = 1.5406 Å (XRD-Philips PW 1730/10) configured in Bragg–Brentano powder diffraction geometry. The analysis of the peak coincidences for each sample was performed using the PDF2 database with license from the International Center for Diffraction Data (ICDD). The measurements of the film electrical conductivity were performed, as a function of temperature, making use of a Keithley 4200 SMU connected to a Jandel four points probe station and a thermal chuck equipped with an electronic temperature controller. The chuck setting temperature was swept from room temperature up to 100 °C, and the actual sample temperature was registered with the help of an additional thermocouple in contact with the sample surface.

3. Results and discussion

The characterization of the films was performed using two sample sets: one with the as-deposited films obtained by RF sputtering at room temperature (25 °C), and the other with the same films after the additional thermal annealing at 475 °C for 3 h. A SEM image of the surfaces obtained for both sample sets can be observed in Fig. 1.

As expected for the sputtering process a good surface uniformity is obtained for the as-deposited films (Fig. 1a), with a particle mean size around 10 nm. After the high temperature annealing process accomplished to obtain films with a single V_2O_5 oxide phase a significant growth of the grain size is observed (>100 nm) (Fig. 1b). Additionally, it can be noted from the grain shapes in Fig. 1b how the film crystallinity is improved as a result of this annealing process [16]. The film structural characterization was carried out using the XRD diffraction technique. With the as-deposited sample set the XRD measurements were performed using a glancing angle configuration in order to obtain diffractograms with high peak resolutions for the expected amorphous thin films. However, a standard powder diffraction configuration was used with the anticipated crystalline samples obtained after the annealing process at 475 °C. In both cases, the sample XRD measurements were corrected in order to eliminate the background XRD spectral contribution due to the substrate. A peak matching analysis was performed in order to match the peaks observed in the resulting XRD diffractograms with the reflection planes included in the PDF2 database records. Peaks matching those of $VO_{0.9}$ were identified in the as-deposited samples, while peaks matching those of the V_2O_5 phase were observed for the annealed samples, as can be seen in diffractograms included in Fig. 2.

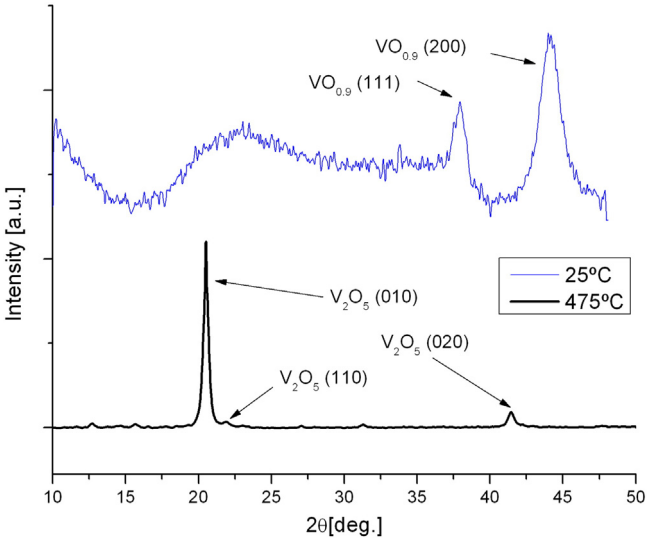

Fig. 2. XRD diffractogram for samples at 25 °C "as deposited", and with thermal annealing at 475 °C.

The electrical measurements performed have provided the behavior of the conductivity σ versus temperature, which is represented in a (log(σ) vs. 1000/T) graph in Fig. 3. These experimental data were fitted by the least squares method using an Arrhenius like equation for conductivity (Eq. (1)). The values obtained for the activation energy ΔW were 0.095 eV for the sample *as deposited* at 25 °C ($VO_{0.9}$), and 0.267 eV for the samples annealed at 475 °C (V_2O_5).

$$\sigma(T) = \sigma_0 \exp(-\Delta W/kT) \quad (1)$$

Finally, the electrical transport mechanism in V_2O_5 thin films is explained on the basis of the small polarons hopping conduction. This transport mechanism is ascertained by fitting the results obtained from the electrical measurements with a model for the electrical conductivity based on the small polaron hopping mechanism described by Mott.

3.1. Charge transport through polarons

Charge transport through polarons is a well known effect observed under strong electron–phonon interaction conditions. The most evident effect of the strong electron–phonon interaction in a material is perceived on the dependency of the electrical conductivity with temperature, but another less obvious effect can also be revealed under this condition, an increase in the effective mass of the electrons due to the dragging of heavy ion nuclei [17]. The set formed by the electron and its associated field deformation is what is known as a polaron. The

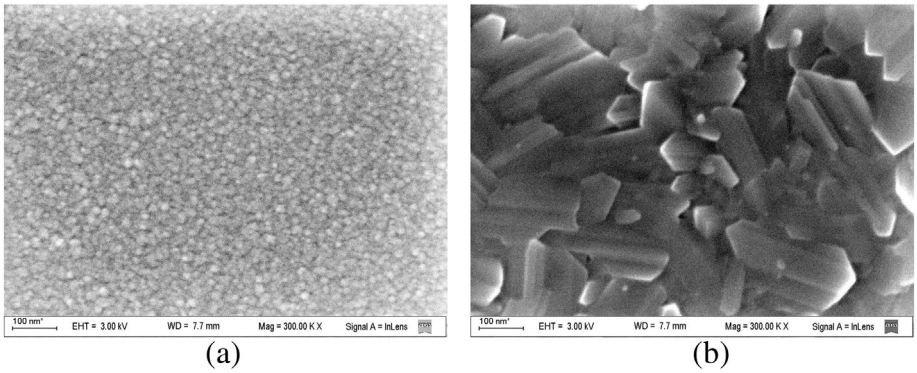

Fig. 1. SEM micrograph of samples a) at 25 °C "as deposited", and b) with thermal annealing at 475 °C.

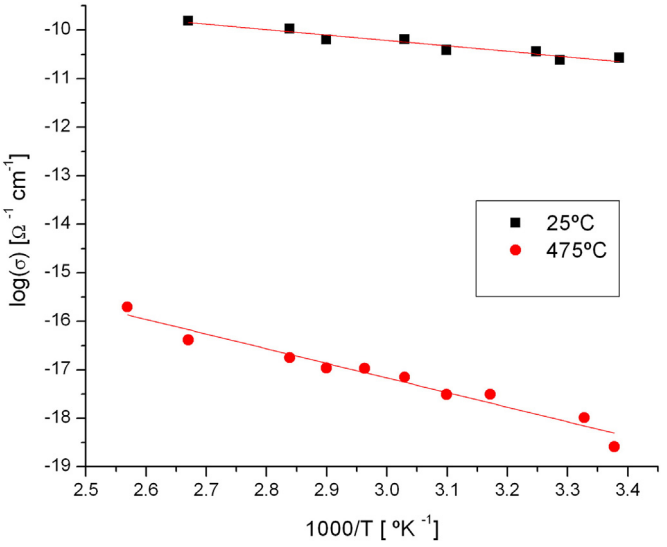

Fig. 3. Measurement of the activation energy ΔW for samples "as deposited" and 475 °C.

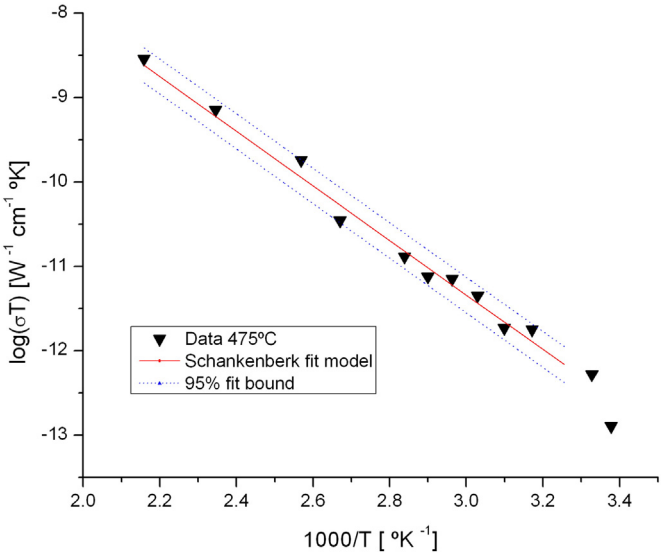

Fig. 4. Small polaron hopping fit using Schnakenberg model on sample 475 °C, with 95% prediction bounds.

main classification of polarons takes into account both the size of the radius with respect to the lattice constant, which gives rise to large or small polarons, and the type of charge transport. While in large polarons charges are moved in a unique band, in small polarons charge remains trapped most of the time on a single ion. The interaction between the lattice vibration and the localized electron induces charges to jump from one atom to a neighboring one. This process is called conduction by hopping charge carriers and takes place through thermal activation at high temperatures [18]. This particular behavior of small polarons remains a candidate to explain charge transport in transition metal oxides [19] like V_2O_5.

In order to verify the nature of the electronic transport mechanism in the V_2O_5 thin films produced the experimental data was fitted by using the Mott–Schnakenberg model. The fitting parameters derived have been used to check the condition for polarons' existence and to identify the particular type of polaron that is responsible of charge transport. Moreover, some of the parameters have been assessed through other alternative equations in order to corroborate the analysis performed.

3.2. Conduction mechanism model

Experimental data were studied using the model developed by Austin–Mott [12,13] for the electrical conductivity of non-crystalline materials and glasses, which considers a conduction mechanism in terms of phonon-assisted hopping of small polarons between localized states. Schnakenberg proposed a simplified formulation for this model taking into account the phonon distribution [14], in which the dependence of the electrical conductivity with temperature can be expressed by Eq. (2) [20]

$$\ln(\sigma T) = \ln(\sigma T)_0 - \frac{W_D}{2kT} - \frac{W_H}{kT}\frac{\tanh(h\nu_0/4kT)}{h\nu_0/4kT} \quad (2)$$

where $(\sigma T)_0$ is a constant, W_D is the activation energy for hopping due to disorder, W_H is the polaron hopping energy and T the temperature in K. Eq. (2) is valid for the hopping of polarons in the non-adiabatic approximation, above the $\theta_D/2$ temperature, where θ_D is the Debye temperature, given by the expression $\theta_D = h\nu_0/k$, where ν_0 is the optical phonon frequency, h is the Planck constant, and k is the Boltzmann constant.

The Schnakenberg equation parameters: σ_0, W_H, W_D and $h\nu_0$ have been evaluated from the fitting of the experimental data shown in the $\log(\sigma T)$ vs. $1000/T$ graph in Fig. 4 using the least-square method. Values obtained with the best line fit, with 95% confidence bounds were: $W_H = 0.1682 \pm 0.0121$ eV, $W_D = 0.2241 \pm 0.0139$ eV and $h\nu_0 = 0.02755 \pm 0.00994$ eV; with a goodness of fit $R^2_{Fit} = 0.9827$. The Debye temperature θ_D computed from $h\nu_0$ was $\theta_D = 319.7$ K.

3.3. Analysis of polarons conduction in V_2O_5

The values of the model parameters obtained from this fitting were used to check the consistency of the several hypotheses established regarding the transport mechanism. First of all, the strong electron–phonon interaction condition was checked by calculating the ratio of the polaron effective mass m_P to the rigid-lattice effective mass m^*. The higher this ratio, the greater the electron–phonon coupling. The ratio between these two parameters was obtained using Eq. (3) [12,13]:

$$m_P = (\hbar^2/2JR^2)exp(\gamma) = m^* exp(\gamma) \quad (3)$$

where J is the bandwidth of the polaron, R is the average spacing between the transition-metal ions, and γ is the electron–phonon interaction parameter, which is given by Eq. (4) [12,13]:

$$\gamma = 2(W_H/h\nu_0). \quad (4)$$

The mass ratio γ evaluated from the previous fitting values, $m_P/m^* = 2.0089 \times 10^5$, corresponds to a $\gamma = 12.2$, which is greater than the value $\gamma > 4$ suggested by Austin–Mott as the limit that indicates the strong electron–phonon interaction in solids [12]. The formation condition for small-polarons was verified using the Emin–Holstein [21] formulation, an inequality that relates the polaron hopping energy W_H with the bandwidth of the polaron J:

$$J < W_H/3. \quad (5)$$

The bandwidth of the polaron J was estimated from the fitting parameters using the approximate expression proposed by Holstein [22]:

$$J \approx 0.67 h\nu_0 (T/\theta_D)^{1/4}. \quad (6)$$

Therefore, the values computed for $J = 0.0182$ eV ($T = 300$ K) and $W_H/3 = 0.0561$ satisfy the small-polaron formation condition in Eq. (5). Once verified the conditions for the strong electron–phonon interaction, and for the existence of small polarons, the type of conduction

mechanisms followed by the charge carriers was established using the condition proposed by Holstein [22] to set the limit between the adiabatic and non-adiabatic regimes [12], given by equation:

$$H = (2kTW_H/\pi)^{1/4}(h\nu_o/\pi)^{1/2}. \quad (7)$$

The polaron conduction regime is determined by the inequality:

$$\begin{cases} J>H & \text{for adiabatic hopping} \\ J<H & \text{for non-adiabatic hopping} \end{cases}.$$

The non-adiabatic hopping regime inequality is satisfied by the values obtained for J and H ($H = 0.0215$ eV) from the fitting parameters. According to Cohen [23], an additional condition must be satisfied in the case of a hopping conduction process. The mobility μ has to be lower than 10^{-2}[cm^2/Vs]. In the case of the non-adiabatic regime the mobility μ can be expressed by Eq. (8) using the model proposed by Murawsky [24]:

$$\mu = (eR^2J^2/\hbar kT)(\pi/4W_HkT)^{1/2}exp(-\Delta W/kT) \quad (8)$$

where R is the vanadium interatomic distance [4], which was experimentally measured in crystalline V_2O_5 [25,26], being 3.55 Å. The mobility obtained using this R value together with the fitting parameters, $\mu = 1.5019 \times 10^{-5}$[cm^2/Vs] meets Cohen condition, suggesting the conduction by polarons hopping in the material under test.

The total activation energy of the material, ΔW, was also evaluated by using the expression suggested by Austin–Mott [12,13]:

$$\begin{cases} \Delta W = W_H + W_D/2 & \text{for } T>\theta_D/2 \\ \Delta W = W_D & \text{for } T<\theta_D/4 \end{cases}. \quad (9)$$

The first equation $\Delta W = W_H + W_D/2$ is the appropriate one for operation at room temperature, taking into account the Debye temperature $\theta_D = 319.7$ K previously evaluated. The activation energy computed from Mott's model parameters, $\Delta W = 0.2803$ eV, fits quite well with the experimental activation energy previously measured from the slope in Fig. 3, $\Delta W = 0.267$ eV.

Table 1 summarizes the different data obtained from the fitting of the experimental measurements of the electrical conductivity with Mott's model, which are compared against similar data reported in literature [3] for single-crystal V_2O_5.

A significant similarity was observed in most of the parameters available for both materials. However, a large difference was reported for the mobility μ, which is two orders of magnitude larger in the case of the V_2O_5 single-crystal. Taking into account the Cohen [23] condition established for the electrical conduction by hopping of charge carriers, which states that this process occurs for mobilities much lower than 10^{-2}[cm^2/Vs], it can be noted that V_2O_5 single crystal (0.15–0.5 $\times 10^{-2}$ cm^2/Vs) is near this limit while V_2O_5 thin-films reported in this work ($\mu = 1.5 \times 10^{-5}$[cm^2/Vs]) are clearly beyond this hoping condition limit. Therefore, the low mobility reported for the V_2O_5 thin-films obtained with the proposed two-stage method suggests that small polarons hopping is the prevailing conduction mechanism in this material.

Table 1
Comparison of material properties for V_2O_5 thin films (current work) and bulk single-crystal (Ioffe [3]). (*) For bulk single crystal WD was computed using Eq. (9) and θ_D as $h\nu_0/k$.

Parameter	V_2O_5 bulk single crystal Ioffe [3]	V_2O_5 thin film this work
ΔW	0.27 eV	0.267 eV
W_H	0.15–0.17 eV	0.1682 eV
W_D	0.2–0.24 eV(*)	0.2241 eV
$h\nu_0$	0.032 eV	0.0275 eV
J	0.01 eV	0.0182 eV
γ	10	12.2
θ_D	371.3 K(*)	319.7 K
μ	0.15–0.5 $\times 10^{-2}$ cm^2/Vs	1.5 $\times 10^{-5}$ cm^2/Vs

3.4. Polaron hopping energy verification

Finally, in order to reinforce the validity of the model employed for the fitting, the polaron hopping energy parameter W_H was also estimated making use of the expression derived from the Austin–Mott [12] model (Eq. (10)),

$$W_H = e^2\left(r_P^{-1} - R^{-1}\right)/4\varepsilon_P \quad (10)$$

where r_p is the polaron radius, and ε_p is the material effective dielectric constant. The r_p value was estimated making use of Eq. (11) proposed by Bogomolov [27] and the interatomic distance between vanadium atoms reported for crystalline V_2O_5, $R = 3.55$ Å [26],

$$r_P = (1/2)(\pi/6)^{1/3}R \quad (11)$$

obtaining a value of $r_P = 1.43$ Å. The other parameter required to obtain W_H, ϵ_p, was estimated using the expression $\epsilon_P^{-1} = (\epsilon_\infty^{-1} - \epsilon_S^{-1})$ [12], where ϵ_S and ϵ_∞ are the static and the high-frequency dielectric constants of the material, respectively. An estimation for the ϵ_S in V_2O_5 provided by [28] ($\epsilon_S = 37.2$) was used, together with an estimate of ϵ_∞ obtained from the V_2O_5 refractive index $N(\epsilon_\infty \sim N^2)$ [4]. N was computed making use of experimental data provided by [29] for the real and imaginary parts of the refractive index, n and k, which corresponds to a value of $N = 2.8$. The W_H value obtained using Eq. (10) with these data reported in literature for V_2O_5, $W_H = 0.1512$ eV, is in good agreement with the hopping energy obtained from the fitting of the experimental conductivity data with Mott's model in Eq. (2), $W_H = 0.1682 \pm 0.0121$ eV.

4. Conclusions and future works

Electrical transport properties of V_2O_5 thin films obtained with a lift-off compatible two-stage process (deposition by sputtering and subsequent annealing) were studied. The structural characterization of the samples by XRD showed peaks matching those of the V_2O_5 phase, confirming that the choice of annealing parameters is suitable to ensure a final pure V_2O_5 phase. The electrical conductivity of the films obtained with this deposition method showed a typical negative exponential behavior with temperature, with a 0.27 eV activation energy for $T > 25$ °C. This temperature dependent conductivity was well explained using the Mott model under the Schnakenberg formulation. A complete set of parameters describing the properties of charge carriers was determined. The consistency of these parameters with the several conditions assumed by Mott's model (strong electron–phonon interaction, existence of small polarons, non-adiabatic regime for the hopping of charge carriers) was checked. The charge carrier parameters are consistent with those reported in literature for single crystal V_2O_5, except the strength of the electron–phonon interaction and the mobility. The much lower mobility observed for the V_2O_5 thin-films due to a stronger electron–phonon interaction fully complies the Cohen condition for driving the hopping of charge carriers, suggesting that small polarons hopping is the main conduction mechanism in V_2O_5 thin films obtained with the deposition method proposed.

Acknowledgments

This work was supported by grant PRH 2007 PFDT No. 203 (PAE 37079), funded by the National Institute of Industrial Technology (INTI) and the National Agency for Promotion of Science, Ministry of Science and Technology of Argentina. The authors also wish to thank Dr. I. Fabregas and Dr. S. Amore XRD for the diffractograms measurements performed on samples.

References

[1] S. Surnev, M. Ramsey, F. Netzer, Vanadium oxide surface studies, Prog. Surf. Sci. 73 (4–8) (2003) 117–165.
[2] V. Eyert, K.-H. Hock, Electronic structure of V_2O_5: role of octahedral deformations, Phys. Rev. B 57 (20) (1998) 12727–12737.
[3] V. Ioffe, I. Patrina, Comparison of the small-polaron theory with the experimental data of current transport in V_2O_5, Phys. Status Solidi 40 (1) (1970) 389–395.
[4] C. Sanchez, R. Morineau, J. Livage, Electrical conductivity of amorphous V_2O_5, Phys. Status Solidi A 76 (2) (1983) 661–666.
[5] J. Bullot, P. Cordier, O. Gallais, M. Gauthier, J. Livage, Experimental determination of the disorder energy in amorphous V_2O_5 layers deposited from gels, Phys. Status Solidi A 68 (2) (1981) 357–361.
[6] N. Izu, G. Hagen, D. Schonauer, U. Roder-Roith, R. Moos, Application of $V_2O_5/WO_3/TiO_2$ for resistive-type SO_2, Sensors 11 (3) (2011) 2982–2991.
[7] K. Hermann, A. Chakrabarti, R. Druzinic, M. Witko, Ab initio density functional theory studies of hydrogen adsorption at the V_2O_5(010) surface, Phys. Status Solidi A 173 (1) (1999) 195–208.
[8] Y. Yang, D. Kim, M. Yang, P. Schmuki, Vertically aligned mixed V_2O_5–TiO_2 nanotube arrays for supercapacitor applications, Chem. Commun. 47 (27) (2011) 7746–7748.
[9] A.-M. Cao, J.-S. Hu, H.-P. Liang, L.-J. Wan, Self-assembled vanadium pentoxide (V_2O_5) hollow microspheres from nanorods and their application in lithium-ion batteries, Angew. Chem. Int. Ed. 44 (28) (2005) 4391–4395.
[10] P.W. Kruse, Uncooled Thermal Imaging: Arrays, Systems, and Applications, SPIE Press, Bellingham, Wash., USA, 2001.
[11] S. Beke, A review of the growth of V2O5 films from 1885 to 2010, Thin Solid Films 519 (6) (2011) 1761–1771.
[12] I. Austin, N. Mott, Polarons in crystalline and non-crystalline materials, Adv. Phys. 18 (71) (1969) 41–102.
[13] N. Mott, Conduction in glasses containing transition metal ions, J. Non-Cryst. Solids 1 (1) (1968) 1–17.
[14] J. Schnakenberg, Polaronic impurity hopping conduction, Phys. Status Solidi B 28 (2) (1968) 623–633.
[15] X. Xu, X. He, G. Wang, X. Yuan, X. Liu, H. Huang, S. Yao, H. Xing, X. Chen, J. Chu, The study of optimal oxidation time and different temperatures for high quality VO_2 thin film based on the sputtering oxidation coupling method, Appl. Surf. Sci. 257 (21) (2011) 8824–8827.
[16] R.W.G. Wyckoff, Crystal Structures, R.E. Krieger Pub. Co., Malabar, Fla, 1982.
[17] C. Kittel, Introduction to Solid State Physics, 8th ed. Wiley, Hoboken, NJ, 2005.
[18] J. T. Devreese, Polarons, arXiv:cond-mat/0004497ArXiv: cond-mat/0004497.
[19] E.A. Davis, N.F. Mott, Conduction in non-crystalline systems v. conductivity, optical absorption and photoconductivity in amorphous semiconductors, Philos. Mag. 22 (179) (1970) 0903–0922.
[20] E. Culea, C. Gheorghiu, A. Nicula, Electrical conductivity of vitreous $75V_2O_5(As_2O_3$–$B_2O_3)$, Phys. Status Solidi A 96 (1) (1986) K85–K88.
[21] D. Emin, T. Holstein, Studies of small-polaron motion IV. Adiabatic theory of the hall effect, Ann. Phys. 53 (3) (1969) 439–520.
[22] T. Holstein, Studies of polaron motion: part I. The molecular-crystal model, Ann. Phys. 8 (3) (1959) 325–342.
[23] M.H. Cohen, Review of the theory of amorphous semiconductors, J. Non-Cryst. Solids 4 (1970) 391–409.
[24] L. Murawski, C. Chung, J. Mackenzie, Electrical properties of semiconducting oxide glasses, J. Non-Cryst. Solids 32 (1–3) (1979) 91–104.
[25] R. Enjalbert, J. Galy, A refinement of the structure of V_2O_5, Acta Crystallogr. Sect. C: Cryst. Struct. Commun. 42 (11) (1986) 1467–1469.
[26] H.G. Bachmann, F.R. Ahmed, W.H. Barnes, The crystal structure of vanadium pentoxide, Z. Krist. 115 (1–2) (1961) 110–131.
[27] V. Bogomolov, E. Kudinov, Y.A. Firsov, Polaron, (Fiz. Tverd. Tela 9 (1967) 3175), Sov. Phys. Solid State 9 (19) (1968) 2502.
[28] P. Clauws, J. Vennik, Lattice vibrations of V_2O_5. Determination of TO and LO frequencies from infrared reflection and transmission, Phys. Status Solidi B 76 (2) (1976) 707–713.
[29] W.R. Folks, J. Ginn, D. Shelton, J. Tharp, G. Boreman, Spectroscopic ellipsometry of materials for infrared micro-device fabrication, Phys. Status Solidi C 5 (5) (2008) 1113–1116.